Measurement: Sensors 18 (2021) 100174

Contents lists available at ScienceDirect

Measurement: Sensors

journal homepage: www.sciencedirect.com/journal/measurement-sensors

Vibration based characterization of tool wearing in micro-milling of ceramics

ARTICLE INFO

Keywords
Ceramics machining
Rake face wearing
Vibration analysis
Feature selection

ABSTRACT

The main aim of the paper is to monitor the micro-milling tool wearing process offline, by a microscopic tool measurement on one hand, and using high-frequency vibration measurement online, during the cutting process, on the other. Relations between the rake face wear stages and the measured online and offline parameters were determined applying an own-developed, artificial neural network based feature selection solution. As the main result, the experiment-based research appoints that measured vibration variable component(s) which characterizes the key, three tool wearing phases in the same way as the real rake face wearing stages occur.

1. Introduction

The main aim of the paper is to monitor the micro-milling tool wearing process offline, by a microscopic tool measurement on one hand, and using high-frequency vibration measurement online, during the cutting process, on the other.

The cycloid or trochoidal form is a milling technology, where the tool milling is going along an arc, avoiding sharp changes in the direction that is especially important in micro-milling of ceramics. Although, it does not control the tool engagement owing to cycloid form, it can reduce the tool load, and can make the optimization of the roughing strategy easier [1]. The problem with the traditional toolpaths is that the tool load increase significantly in the corners requiring shallower depths of cut and reduced feed. This problem can be avoided with cycloid and wave form paths. Since the experimental test machining unit, called pocket, as a small geometry to eliminate it from the base material by micro-milling not had circle geometry, the technology was optimized with entremets, which is an option in the tool control software to reduce the tool load in the corners [1,2].

The effect of having smaller radial cutting forces increases the stability of the cut, i.e., there is a substantial decrease in the force for pushing the tool to the workpiece and in the vibration level as well. While increasing the cutting speed and reducing chip thickness, the heat generated at the cutting point is reduced, so it is possible to increase the cutting depth further. These positively changed milling conditions ensure that the tool and the machine are more wear-resistant, exhibiting a much longer service life, and the machining process thus becomes very effective and desirable in many new applications [3–5]. This technology can be applied to produce deep grooves, pockets or high workpiece sides, with high process reliability and long tool life [6–8].

In the previous paper of the authors, the process of tool wearing was investigated by direct and indirect methods in relation to the different CAM (Computer Aided Manufacturing) toolpaths [9,10]. These research results concluded that the nature of the volume change of the manufactured pockets can be accurately traced by an engineering feature calculated on the basis of the workpiece connected vibration measurement series:

- Number of the times the vibration signal crosses its mean value (1):

$$\sum \left(sgn(x(i) - \bar{x}) \neq sgn(x(i+1) - \bar{x}) \right) \quad (1)$$

Fig. 1 shows the almost identical change in the micro-milling tool wear described by the changes in the volume of the machined pockets and the vibration based, calculated variable appointed by the feature selection method [11]. Based on the graph, one can recognize that the two diagrams behave almost identical, consequently, the actual status of the tool lifetime can be well monitored with vibration-based diagnostics method in micro-milling of ceramics. After sufficient number of measurements and experiments, the tool monitoring can be automatized during ceramics micro-milling, and finally, the system could be optimized.

The aims of the paper are – continuing a previous research of the authors [10] – to concentrate only on one kind of diagnostics of rake face wearing of the micro-milling tool angles in machining of ceramics and to determine the relationships between the related cutting vibration and the rake face wear of the tool. Finally, the two rake faces can be diagnosed separately and individually.

2. Rake face wear of the cutting tool

Micro-milling tools were applied for the cutting experiments on ceramics (Fig. 2). Such tools, which have zero or negative rake angles, should be chosen for cutting the given kind of brittle materials.

Measurements were performed using Zeiss Discovery V8 microscope and based on the taken pictures the authors evaluated the wearing. The tool was applied until its breakage, this cycle of measurements covered the entire tool lifetime resulting in various identified phenomena.

Asymmetrical wear of the cutting edges was observed during tool lifetime. This phenomenon was also observed in the previous research of the authors, too, where the waveform strategy was investigated in cutting of ceramics material [9].

During the experiments, it was not possible to take microscopic

https://doi.org/10.1016/j.measen.2021.100174

Available online 23 September 2021

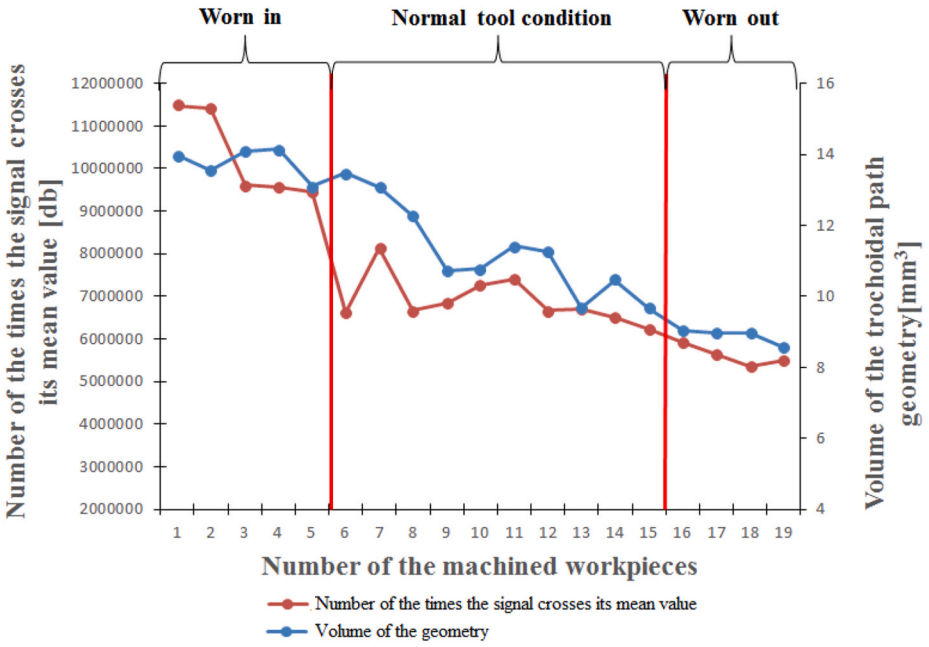

Fig. 1. Applying the trochoidal toolpath, the similar behaviour between the measured vibration signal based, selected engineering feature and the change in the micro-milling tool wear described by the changes in the volume of the machined pockets [10].

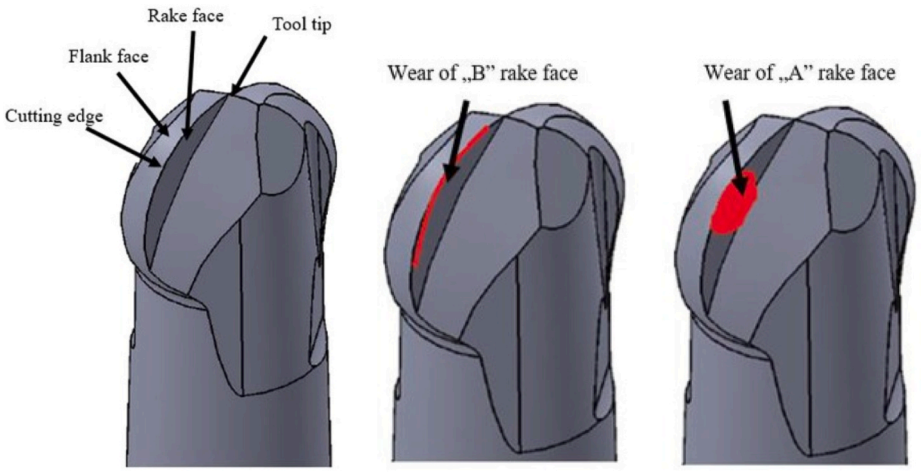

Fig. 2. Micro-milling tool geometry in 3D view and the most important wearing places at the early tool life period.

photos after every machining, thus, these were taken after every 5th pocket. Based on these measurements, the different rake face stages of the micro ball mill can be determined, at the first checkpoint in Fig. 3. It was observed that while one of the rake faces began to wear, the other cutting edge remained intact. Up to the 3rd checkpoint, this difference was continuous, but the extent of the difference decreased. At the 4th checkpoint the tool edges have become equally unusable.

After determining the wear curves, it was necessary to find the boundary points where the worn-in and the linear wear stages of the cutting edges ended (followed by the and worn-out stage until the break) as specified by the Taylor curve. Having defined these thresholds, the rake face wear stages can be differentiated for each machining along the entire tool lifetime, Consequently, the individual micro-cutting machining were ordered to these three, different classes (worn-in, normal, wear-out). After these classes and their machining members have been defined, the next step was to apply the feature selection method (FS) developed by some of the authors [11]. It was applied to find the most descriptive statistical/engineering features for distinguishing the three different stages of the tool life. Additionally, the frequency values of the vibration signal where also analysed to separate the classes of the Taylor curve from each other (as feature selection in frequency domain).

3. Vibration diagnostics using the feature selection method

3.1. Analysis of engineering features for the "A" rake face

Analysing the "A" rake face (Fig. 2), as result, the algorithm identified that the mean value of the vibration signal and the number of the times the signal crosses the mean value calculated at each workpiece can differentiate the three stages of the rake face tool wear.

Based on the Taylor curves, the worn in phase of "A" rake face ends at 5th pocket, while the normal wear range ends at 13th pocket. The graph in Fig. 4 shows that the mean values decrease to 5th pocket and after then a break point is observed.

In the normal wear range, a steeper drop is observed than in the

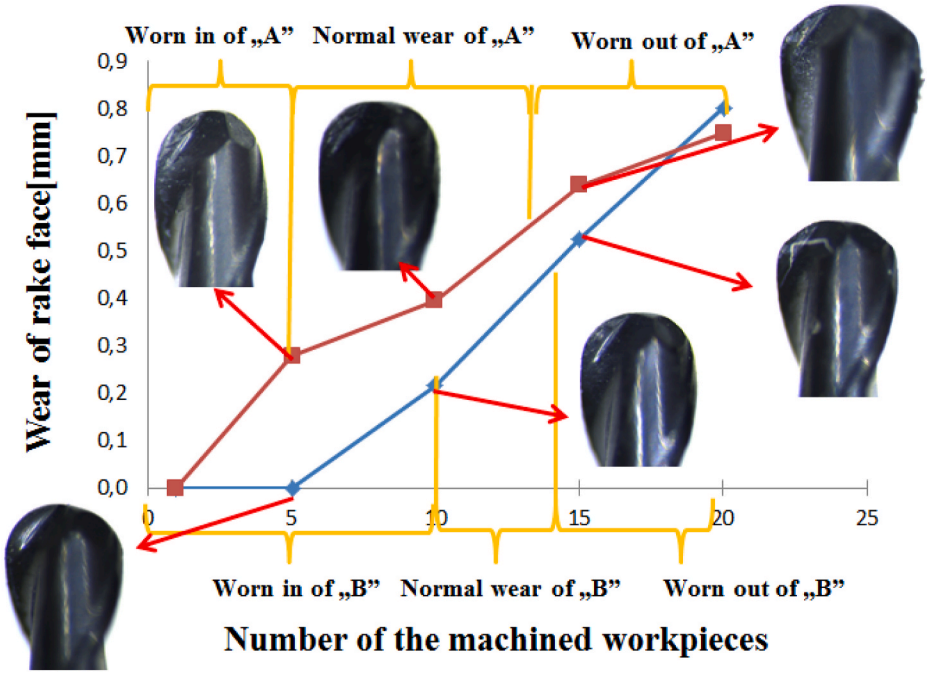

Fig. 3. Different behaviour of “A” and “B” wear of rake faces during trochoidal toolpath micro-milling of ceramics.

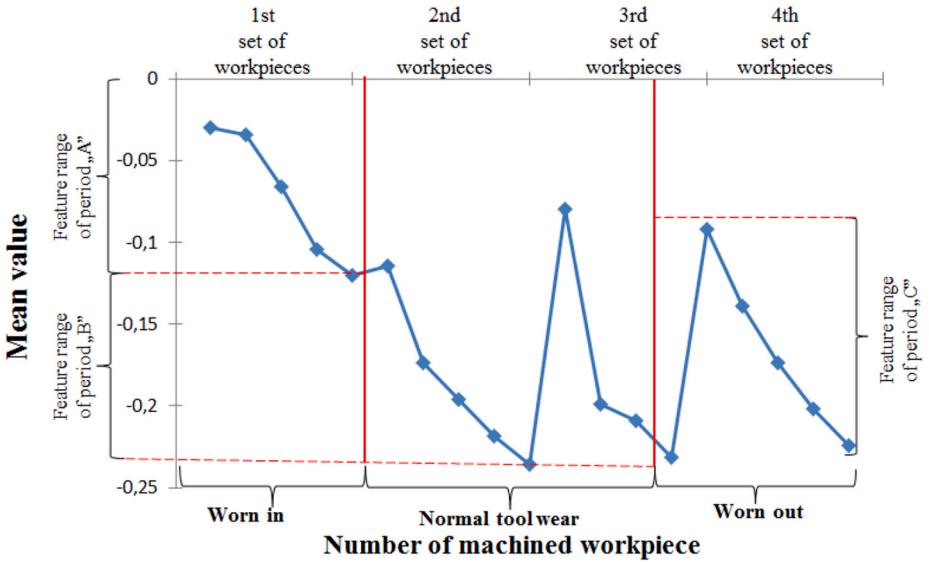

Fig. 4. Mean values as a function of the manufactured workpieces analysing the “A” rake face.

worn-in section. The average values range extends from −0.2 to −0.24, apart from th11th pocket. The tool enters the worn-out range from 14th pocket. However, it can be seen in Fig. 4 that a sudden jump occurs at the 15th value. However, this value is the transition point to the worn-out range of the “B” rake face.

Based on the Taylor curve and on the curve of the change in the average values (Fig. 5.), it can be stated that the whole tool enters the worn-out phase between the 14–15th pockets. In the case of the second analysed statistical/engineering feature represented in Fig. 5, the normal wear phase is well separated from the worn-in phase. In the worn-out phase, a gradual decrease of the related values is observed.

3.2. Analysis of engineering features for the “B” rake face

Analysing the “B” rake face, as result, the FS algorithm identified that the mean value calculated at each workpiece can differentiate the three stages of the tool wear. The “B” rake face enters in the normal wear range at the 10th pocket where a breaking point is observed. The cutting tool enters the worn-out range at the 15th pocket, where another jump is observed at the data set values, like at the “A” rake face represented in Fig. 4.

3.3. Analysis of frequency features for the “A” rake face

The use of above described statistical/engineering feature-based selection can be extended to monitor the wear of a complex tool angle system.

Thus, the previously applied method was extended by the frequency feature selection (FFS) method. Using FFS, the characteristic frequencies of the signal can be determined in which the rake face wear stages

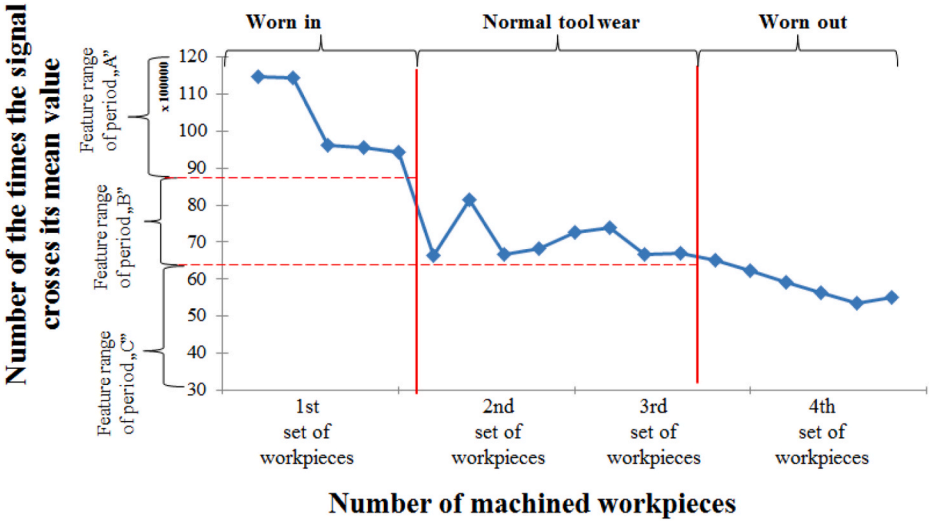

Fig. 5. Number of the times the signal crosses its mean value as a function of the manufactured workpieces analysing the "A" rake face.

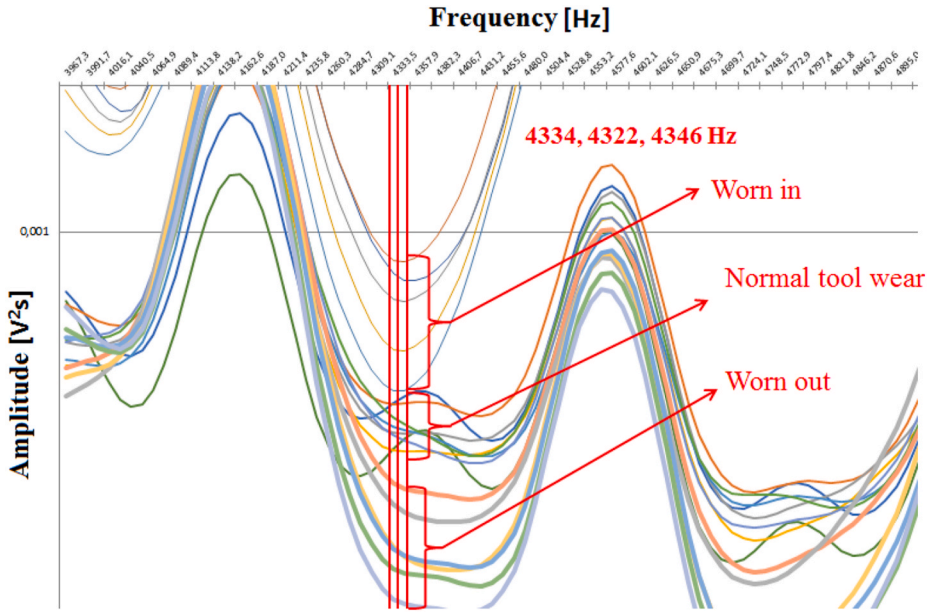

Fig. 6. Separation of the sharp (thin curves), normal (middle sized curves) and worn (thick curves) tool at 4.3 kHz analysing the "A" rake face.

change.

According to FFS calculations, the separation of the wear ranges at the "A" rake face occurs around 4.3 kHz. The results, as separated frequency domain amplitude curves, are shown in Fig. 6.

Based on Fig. 6, the tool life stages are well separable. Furthermore, as the tool wear increases, the amplitude decreases. This is probably due to the continuous decrease in the contact area between the tool and the workpiece.

3.4. *Analysis of frequency features for the "B" rake face*

In the case of "B" rake face, the separation of the three stages of the Taylor curve is observed at 6068Hz (Fig. 7) as separated frequency domain amplitude curves.

At the "B" rake face, the values of the amplitudes in the worn-in range are low and constant (Fig. 8), in the normal wear range the values suddenly jump, and then return to low values in the worn-out range.

4. Conclusions

The preliminary research results of the authors [1,9] mirrored that the wear of the micro-milling tool in machining ceramics can be well monitored by considering the volume of the formed pockets. However, to gain a deeper understanding of this process, the result in the diagnostics in the wearing of each cutting-edge angles are presented in the paper. The purpose was to find a relationship between the wear of cutting-edge angles and the vibrations signals.

During the tests, it was found that the cutting edges and the tool faces show asymmetric wear when using a trochoidal toolpath. Examining the statistical/engineering vibration signal features resulted that the change in the mean values and the number of the times the signal crosses the mean value of the measured signal successfully describes the complex wearing course for each cutting edges. Additionally, analysing the signal vibration in the frequency domain resulted that the amplitudes at 4.3 and 6 kHz represents the complete separation of the worn-in, normal and wear out stages of the "A" and "B" rake faces, respectively. Finally, the two rake faces can be diagnosed separately and individually.

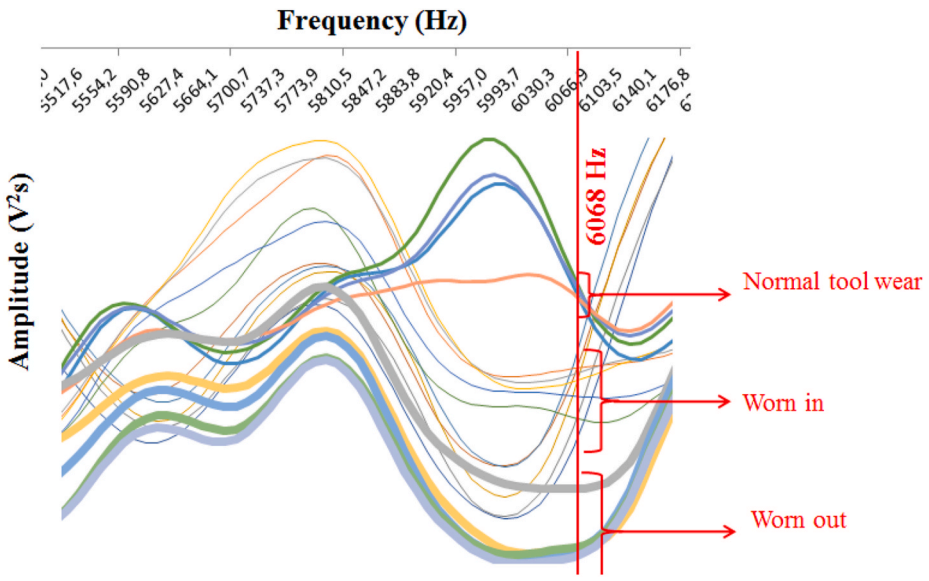

Fig. 7. Separation of the sharp (thin curves), normal (middle sized curves) and worn (thick curves) tool at 6 kHz. analysing the "B" rake face.

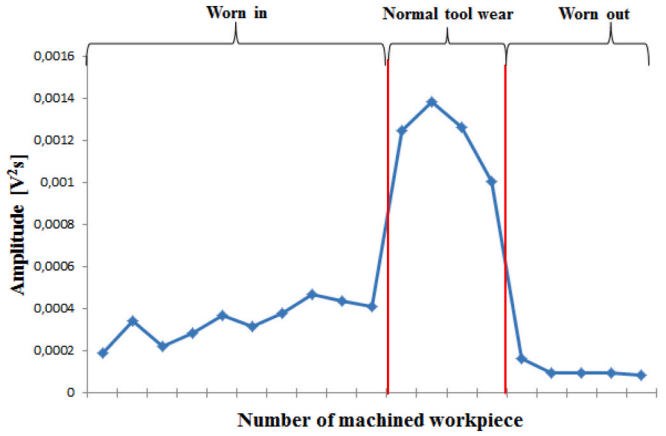

Fig. 8. Amplitude value change in relation to the tool wear stages at 6 kHz, analysing the "B" rake face.

All these results represent the really complex and diverse tool wearing behaviour of micro-milling tools, considering the different cutting edges.

Acknowledgements

The research in this paper was partly supported by the European Commission through the H2020 project EPIC (https://www.centre-epic.eu/) under grant No. 739592 and by the Hungarian ED_18-2-2018-0006 grant on a "Research on prime exploitation of the potential provided by the industrial digitalization" (https://inext.science/).

References

[1] L. Móricz, Zs J. Viharos, A. Németh, A. Szépligeti, Efficient ceramics manufacturing through tool path and machining parameter optimisation, in: 15th IMEKO TC10 Workshop on Technical Diagnostics: "Technical Diagnostics, Cyber-Physical Era", Budapest, Hungary, 2017, pp. 143–148.

[2] L. Móricz, Zs J. Viharos, A. Németh, A. Szépligeti, "Indirect measurement and diagnostics of the tool wear for ceramics micro-milling optimisation", *XXII IMEKO World Congress*, J. Phys. Conf. 1065 (2018) paper ID: 102003.

[3] M. Šajgalík, M. Kušnerová, M. Harni, J. Valí, A. Czán, T. Czánová, M. Drbúl, M. Borzan, J. Kmec, Analysis and prediction of the machining force depending on the parameters of trochoidal milling of hardened steel, Appl. Sci. 10 (No. 5) (2020) paper ID: 1788.

[4] J. Santhakumar, U. Mohammed Iqbal, Parametric optimization of trochoidal step on surface roughness and dish angle in end milling of AISID3 steel using precise measurements, Materials 12 (2019) paper ID: 1335.

[5] P. Amaro, P. Ferreira, F. Simoes, Tool wear analysis during duplex stainless steel trochoidal milling, AIP Conf. Proc. 1960 (2018) paper ID: 070001, 2018.

[6] K. Xu, B. Wu, Z. Li, K. Tang, Time-E_cient trochoidal tool path generation for milling arbitrary curved slots, J. Manuf. Sci. Eng. 141 (2019). Nr. 3., paper ID: 031008.

[7] A. Pleta, D. Ulutan, L. Mears, Investigation of trochoidal milling in nickel-based superalloy inconel 738 and comparison with end milling, in: ASME 2014 International Manufacturing Science and Engineering Conference Collocated with the JSME 2014, Proceedings of the International Conference on Materials and Processing and the 42nd North American Manufacturing Research Conference, Detroit, MI, USA, 9–13 June 2014 vol. 2, American Society of Mechanical Engineers, New York, NY, USA, 2014 paper ID: MSEC2014-4151, V002T02A058.

[8] F. Bettine, H. Ameddah, H.R. Manna, A neural network approach for predicting kinematic errors solutions for trochoidal machining in the matsuura MX-330 five-Axis machine, FME Trans 46 (2018) 453–462, 2018.

[9] L. Móricz, Zs J. Viharos, A. Németh, A. Szépligeti, M. Büki, Off-line geometrical and microscopic & on-line vibration based cutting tool wear analysis for micro-milling of ceramics, Measurement 163 (2020) paper ID: 108025.

[10] L. Móricz, Zs J. Viharos, M. Büki, Effect of CAM path strategies on tool life in ceramics micro-cutting, in: *17th IMEKO TC 10 and EUROLAB Virtual Conference: "Global Trends in Testing*, Diagnostics & Inspection for 2030, 2020, ISBN 978-92-990084-6-1, pp. 92–98. October 20-22., 2020.

[11] Zs J. Viharos, K.B. Kis, Á. Fodor, M. Büki, Adaptive, hybrid feature selection (AHFS), Pattern Recogn. 116 (2021). Paper nr. 107932.

László Móricz
University of Pannonia, Faculty of Engineering, Mechatronic Education and Research Institute, Zalaegerszeg, Hungary
E-mail address: moricz1888@gmail.com.

Zsolt János Viharos*
Institute for Computer Science and Control (SZTAKI), Centre of Excellence in Production Informatics and Control, Center of Excellence of the Hungarian Academy of Sciences (HAS), Eötvös Loránd Research Network (ELKH), Budapest, Hungary
John von Neumann University, Kecskemét, Hungary

* Corresponding author.
E-mail address: viharos.zsolt@sztaki.hu (Z.J. Viharos).